Communications in Mathematics and Applications
Vol. 16, No. 2, pp. 615–629, 2025
ISSN 0975-8607 (online); 0976-5905 (print)
Published by RGN Publications
DOI: 10.26713/cma.v16i2.3052

http://www.rgnpublications.com

Research Article

An Analytical Approach for a Deterministic Epidemiological Model – Monkeypox Clinical Disease

J. Sujatha*, N. Magesh and G. Tamil Preethi

Post-Graduate and Research Department of Mathematics, Government Arts College for Men, Krishnagiri 635001, Tamilnadu, India
***Corresponding author:**sujiselva8815@gmail.com

Received: February 19, 2025 **Revised:** April 4, 2025 **Accepted:** May 21, 2025

Abstract. In this study, we investigate a non-linear differential equation modeling the transmission dynamics of monkeypox. We begin with a thorough stability analysis to assess the equilibrium points of the model, providing insights into the conditions under which the disease may persist or diminish within a population. Following this, we employ the q-*Homotopy Analysis Transform Method* (q-HATM) to derive analytical solutions, showing its effectiveness in handling the complexities inherent in non-linear systems. Our findings reveal that while both methods yields valuable insights into the behavior of the monkeypox transmission model, q-HATM offers greater flexibility in terms of initial conditions and non-linearity. This work contributes to the understanding of monkeypox for future research in disease modeling using advanced mathematical techniques.

Keywords. Stability analysis, Monkeypox, Epidemic model, Nonlinear differential equations, Mathematical models, q-Homotopy analysis transform method

Mathematics Subject Classification (2020). 37M05, 34F05, 92D30

1. Introduction

In recent years, the study of fractional differential equations has garnered significant attention due to their applications in various fields such as physics, engineering, and finance. These equations allow for more accurate modeling of real-world phenomena by incorporating memory and hereditary properties. Among the various methods developed to solve fractional differential equations. The resurgence of infectious diseases, such as monkeypox, underscores

the importance of developing robust mathematical models to understand their dynamics. In 1958, (Chowell *et al*. [7]) the virus that causes monkeypox was discovered in Denmark in study monkeys. In Congo (Kinshasa), (Reynolds *et al*. [18]), a nine-month-old boy contracted mpox in 1970, the first known human case. After smallpox was eradicated in 19800s and the pox vaccine was paused globally, mpox gradually expanded throughout Africa (Chowell *et al*. [7]). Mpox has since been reported sporadically in West Africa (Clade II) and central and eastern Africa (Clade I) (Chowell *et al*. [7]). An epidemic in the United States in 2003 was linked to imported wild animals (Clade II) (Chowell *et al*. [7]). Since 2005, Congo (Kinshasa) has seen thousands of cases reported annually (Thornhill *et al*. [21]). Mpox resurfaced in Nigeria in 2017 (Somma *et al*. [20]) and is still spreading among Nigerians and tourists visiting other countries. Congo (Kinshasa) has also seen a rise in mpox infections and fatalities since 2022 (Thornhill *et al*. [21]). Clade II, a recent offshoot of Clade I, has been spreading from person to person in several parts of the nation (Vivancos *et al*. [24]). The clade has also been detected in other nations as of mid-2024 (Hobson *et al*. [8], Huo *et al*. [9], and Johnson *et al*. [10]).

Treating the rash, controlling discomfort, and avoiding complications are the main objectives of mpox treatment. To assist manage symptoms and prevent more issues, early and supportive care is crucial. A painful rash is a symptom of the viral infection known as monkeypox. After a few weeks, the majority of people recover without treatment. People can occasionally get terribly sick and pass away. Symptoms often appear 7-10 days after an individual is infected to the mpox virus. Scarring from the skin rash and, in cases where the eyes are involved, perhaps permanent vision loss are the most frequent long-term complications. which can cause corneal injury. Monkeypox primarily affects the skin and mucous membranes, leading to symptoms such as skin lesions, fever and chills, lymphadenopathy, respiratory symptoms.

Although there are currently no proven cures for mpox infection, the disease can be stopped from spreading by using a variety of innovative antivirals, including tecovirimat, vaccinia immune globulin, and brincindofovir. In the past ten years, monkeypox has significantly increased in tandem with a decline in smallpox herd immunity. Although the smallpox vaccine has been demonstrated to be 85% effective in preventing monkeypox, it is no longer routinely available due to the smallpox eradication worldwide. The disease can be prevented or its severity reduced with the use of the post-exposure vaccine. The illness has received little attention in the past, which has led to a lack of understanding regarding its mechanisms of transmission. However, few studies have attempted to use a mathematical modelling technique to study the dynamics of the monkeypox virus. Predicting outbreaks, directing public health measures, and influencing policy decisions all depend on accurate modelling (Somma *et al*. [20]).

In this context, fractional differential equations have emerged as powerful tools due to their ability to incorporate memory effects and capture complex behaviors in biological systems. A critical aspect of modeling infectious diseases is stability analysis, which examines how solutions to mathematical models respond to perturbations. Stability ensures that small changes in initial conditions or parameters do not lead to unpredictable or chaotic outcomes (Alzahrani and Zeb [3], and Huo *et al*. [9]), which is vital for reliable predictions in epidemiological studies. This paper focuses on advanced methodology for solving FDEs the q-HATM. The q-HATM employs a homotopy approach to construct approximate solutions, allowing for significant flexibility in addressing non-linear dynamics often observed in disease spread. This method facilitates the exploration of solution space and provides insights into the stability of the model (Padmavathi *et al*. [12], and Veeresha *et al*. [22, 23]).

On the other hand, the q-HATM offers a novel perspective by extending classical calculus concepts to fractional orders (Padmavathi *et al*. [12, 13], Pathak, *et al*. [14], Prakash and Kaur [15, 16], Prakash *et al*. [17], Reynolds *et al*. [18], Singh *et al*. [19], Somma *et al*. [20], Thornhill *et al*. [21], Veeresha *et al*. [22, 23], Vivancos *et al*. [24], and Youssef *et al*. [25]). This approach maintains the intuitive properties of traditional differential equations while accommodating fractional derivatives, making it particularly suitable for modeling phenomena with memory effects, such as the transmission dynamics of monkeypox. By comparing these two methods, this study aims to evaluate their effectiveness in capturing the stability characteristics of monkeypox models. The analysis will highlight how each method addresses non-linearity and stability, providing valuable insights into their applicability for epidemiological modeling (Abdullah *et al*. [1], Alkunle *et al*. [2], Alzahrani and Zeb [3], Atangana and Gómez-Aguilar [4, 5], and Bhunu and Mushayabasa [6]). Ultimately, this research seeks to enhance our understanding of monkeypox transmission dynamics and contribute to more effective public health strategies.

2. Model Formulation

A deterministic compartment model on the transmission dynamics of the Monkeypox disease is been proposed. The total population is divided into six compartments, susceptible $\mathscr{A}(\mathrm{t})$, exposed $\mathscr{B}(\mathrm{t})$, infected $\mathscr{C}(\mathrm{t})$, systemic issues $\mathscr{Y}(\mathrm{t})$, rashes $\mathscr{Z}(t)$, recovered $\mathscr{R}(\mathrm{t})$ such that $\mathscr{N}(\mathrm{t}) = \mathscr{A}(\mathrm{t}) + \mathscr{B}(\mathrm{t}) + \mathscr{C}(\mathrm{t}) + \mathscr{Y}(\mathrm{t}) + \mathscr{Z}(\mathrm{t}) + \mathscr{R}(\mathrm{t})$. Recruitment into human population is at a rate θ is a birth rate, transmission rate β is the rate at which susceptible individuals become exposed upon contact with infected individuals, the latent period rate σ is the rate at which exposed individuals become infectious, recovery rate γ the rate at which infected individuals recover, systemic issue development rate s the rate at which infected individuals experience systemic issues, rash development rate δ the rate at which systemic issues develop a rash, rash recovery rate r the rate at which individuals recover from rash symptoms and natural death occurs in the human population at rate μ.

The transition among various compartment considered in the model is governed by the following set of non linear differential equation below:

$$\begin{aligned}
\frac{d\mathscr{A}}{dt} &= \theta - \beta\,\mathscr{A}(\mathrm{t})\,\mathscr{C}(\mathrm{t}) - \mu\,\mathscr{A}(\mathrm{t});\\
\frac{d\mathscr{B}}{dt} &= \beta\,\mathscr{A}(\mathrm{t})\,\mathscr{C}(\mathrm{t}) - \sigma\,\mathscr{B}(\mathrm{t}) - \mu\,\mathscr{B}(\mathrm{t});\\
\frac{d\mathscr{C}}{dt} &= \sigma\,\mathscr{B}(\mathrm{t}) - \gamma\,\mathscr{C}(\mathrm{t}) - s\,\mathscr{C}(\mathrm{t}) - \mu\,\mathscr{C}(\mathrm{t});\\
\frac{d\mathscr{Y}}{dt} &= s\,\mathscr{C}(\mathrm{t}) - \delta\,\mathscr{Y}(\mathrm{t}) - \mu\,\mathscr{Y}(\mathrm{t});\\
\frac{d\mathscr{Z}}{dt} &= \delta\,\mathscr{Y}(\mathrm{t}) - r\,\mathscr{Z}(\mathrm{t}) - \mu\,\mathscr{Z}(\mathrm{t});\\
\frac{d\mathscr{R}}{dt} &= \gamma\,\mathscr{C}(\mathrm{t}) + r\,\mathscr{Z}(\mathrm{t}) - \mu\,\mathscr{R}(\mathrm{t}),
\end{aligned} \tag{1}$$

where the parameter values are $\beta = 2.0/10^9$, $\delta = 0.004$, $\sigma = 0.01$, $\gamma = 0.002$, $\theta = 2300$, $\mu = 3.0/10^5$, $s = 0.005$, $r = 0.001$ and the initial values are $\mathscr{A}(0) = 34218169$, $\mathscr{B}(0) = 5000$, $\mathscr{C}(0) = 1720$, $\mathscr{Y}(0) = 157$, $\mathscr{Z}(0) = 120$, $\mathscr{R}(0) = 99$. Using the initial and parametric values, the model of the fractional-order dynamical system represented mathematically.

3. The Role of Feedback in Achieving Stability

In this section, we conduct a comprehensive stability analysis of the proposed system to evaluate its robustness and responsiveness to perturbations. The stability of the system is primarily assessed using Hartman-Grobman theorem, which provides a systematic approach to ascertain characteristics. We begin by identifying the equilibrium points of the system (1).

3.1 Monkeypox-Free Equilibrium State

The disease free equilibrium point represents a state in which the disease is absent from the population. In our model, this equilibrium is characterized by the absence of infected individuals, leading to a stable population of susceptible individuals. Mathematically, we denote this equilibrium by the condition $\mathscr{C} = 0$, where $\mathscr{C}$ represents the number of infected individuals. For the monkeypox free equilibrium state E_0,

$$E_0 = \left(\frac{\theta}{\mu}, 0, 0, 0, 0, 0\right).$$

The Jacobian of the system (1) is given by,

$$J = \begin{bmatrix} -\beta\mathscr{C} - \mu & 0 & -\beta\mathscr{A} & 0 & 0 & 0 \\ \beta\mathscr{C} & -\sigma - \mu & \beta\mathscr{A} & 0 & 0 & 0 \\ 0 & \sigma & -\gamma - s - \mu & 0 & 0 & 0 \\ 0 & 0 & s & -\delta - \mu & 0 & 0 \\ 0 & 0 & 0 & \delta & -r - \mu & 0 \\ 0 & 0 & \gamma & 0 & r & -\mu \end{bmatrix}.$$

The value of $J(E_0)$ is given by,

$$J(E_0) = \begin{bmatrix} -\mu & 0 & -\frac{\beta\theta}{\mu} & 0 & 0 & 0 \\ 0 & -\sigma - \mu & \frac{\beta\theta}{\mu} & 0 & 0 & 0 \\ 0 & \sigma & -\gamma - s - \mu & 0 & 0 & 0 \\ 0 & 0 & s & -\delta - \mu & 0 & 0 \\ 0 & 0 & 0 & \delta & -r - \mu & 0 \\ 0 & 0 & \gamma & 0 & r & -\mu \end{bmatrix}.$$

The transmissions matrix F and transition matrix V can be given as:

$$F = \begin{bmatrix} \frac{\beta\theta}{\mu} & 0 \\ 0 & 0 \end{bmatrix} \quad \text{and} \quad V = \begin{bmatrix} \gamma + s + \mu & 0 \\ -\gamma & \mu \end{bmatrix}.$$

Now, after much elucidation we obtain the next generation matrix as

$$FV^{-1} = \begin{bmatrix} \frac{\beta\theta}{\mu(\gamma+\mu+s)} & 0 \\ 0 & 0 \end{bmatrix}.$$

Hence the reproduction number is defined as the largest eigenvalue of the next generation matrix FV^{-1} and can be obtained as:

$$R_0 = \frac{\beta\theta}{\mu(\gamma + \mu + s)}.$$

3.2 Endemic Equilibrium State

When both susceptible and infected individuals are present and the disease remains at a steady level in the community, this is known as the endemic equilibrium point. A constant predominance of the disease results from this equilibrium, where the number of new infections balances with recoveries and other transitions. The Hartman-Grobman theorem, which offers a framework for comprehending the behaviour of dynamical systems close to equilibrium points, can be used to examine the stability of this endemic equilibrium.

The Jacobian matrix about the endemic equilibrium is given as:

$$J = \begin{bmatrix} \mathfrak{d}_{11} & 0 & \mathfrak{d}_{13} & 0 & 0 & 0 \\ \mathfrak{d}_{21} & \mathfrak{d}_{22} & \mathfrak{d}_{23} & 0 & 0 & 0 \\ 0 & \mathfrak{d}_{32} & \mathfrak{d}_{33} & 0 & 0 & 0 \\ 0 & 0 & \mathfrak{d}_{43} & \mathfrak{d}_{44} & 0 & 0 \\ 0 & 0 & 0 & \mathfrak{d}_{54} & \mathfrak{d}_{55} & 0 \\ 0 & 0 & \mathfrak{d}_{63} & 0 & \mathfrak{d}_{65} & \mathfrak{d}_{66} \end{bmatrix}.$$

Here, $\mathfrak{d}_{11} = -\beta\mathscr{C} - \mu$, $\mathfrak{d}_{13} = -\beta\mathscr{A}$, $\mathfrak{d}_{21} = \beta\mathscr{C}$, $\mathfrak{d}_{22} = -\sigma - \mu$, $\mathfrak{d}_{23} = \beta\mathscr{A}$, $\mathfrak{d}_{32} = \sigma$, $\mathfrak{d}_{33} = -\gamma - s - \mu$, $\mathfrak{d}_{43} = s$, $\mathfrak{d}_{44} = -\delta - \mu$, $\mathfrak{d}_{54} = \delta$, $\mathfrak{d}_{55} = -r - \mu$, $\mathfrak{d}_{63} = \delta$, $\mathfrak{d}_{65} = r$, $\mathfrak{d}_{66} = -\mu$.

According to the Hartman-Grobman theorem, if we have an equilibrium point in a nonlinear system, we can examine the local behavior of the system by linearizing it around that point. Specifically, for our endemic equilibrium $(\mathscr{A}^*, \mathscr{C}^*)$, where $\mathscr{A}^*$ is the number of susceptible individuals and $\mathscr{C}^*$ is the number of infected individuals, we can derive the Jacobian matrix J of the systems equations at this equilibrium.

The eigenvalues of this Jacobian matrix play a crucial role in determining the stability of the endemic equilibrium. If all the eigenvalues are negative real part (especially in a main diagonal matrix) then the endemic equilibrium is locally asymptotically stable.

According to the Hartman-Grobman theorem, we may therefore conclude that the characteristics of the Jacobian matrix produced for our system of differential equations to the endemic equilibrium determine its local stability, which is locally asymptotically stable.

4. A Novel Framework for Advanced q-HATM Solutions

This chapter introduces a novel framework called the advanced *q-Homotopy Analysis Transform Method* (q-HATM) which aims to address these challenges by providing a sophisticated analytical tool for modelling the dynamics of monkeypox. We begin by exploring the theoretical foundations and basic well known definitions of q-HATM.

Definition 4.1. The fractional R-L derivative of a function $f(\iota)$ is determined as

$$J^{\wp}(f(\iota)) = \frac{1}{\Gamma(\wp)} \int_0^{\iota} (\iota - \varrho)^{\wp - 1} (f(\varrho))\, d\varrho. \tag{2}$$

Definition 4.2. Here is the presentation of $f \in C_{-1}^{n}$ is Caputo fractional order derivative,

$$D_{\iota}^{\wp}(f(\iota)) = \begin{cases} \frac{d^m f(\iota)}{d\iota^m}, & \text{if } \wp = m \in \mathbb{N}, \\ \frac{1}{\Gamma(m-\wp)} \int_0^{\iota} (\iota - \varrho)^{m-\wp-1} (f^m(\varrho))\, d\varrho, & \text{if } m-1 < \wp < m,\ m \in \mathbb{N}. \end{cases} \tag{3}$$

Definition 4.3. The LT of $f(\iota)$ with respect to fractional Caputo derivative is

$$\mathcal{L}[D_{\iota}^{\wp}(f(\iota))] = s^{\wp}F(s) - \sum_{r=0}^{m-1} s^{\wp-r-1}f^{(r)}(0+) \quad (m-1 < \wp \le m), \tag{4}$$

where $F(s)$ is LT of $f(\iota)$. For more definitions and properties of q-HATM, one can refer, Padmavath *et al*. [12], Prakash and Kaur [15, 16], and Veeresha *et al*. [22, 23].

4.1 Application of q-HATM

Consider the system of equations of fractional order

$$\begin{aligned}
&D_t^{\phi}\mathscr{A}(\mathrm{t}) = \theta - \beta\,\mathscr{A}(\mathrm{t})\,\mathscr{C}(\mathrm{t}) - \mu\,\mathscr{A}(\mathrm{t});\\
&D_t^{\phi}\mathscr{B}(\mathrm{t}) = \beta\,\mathscr{A}(\mathrm{t})\,\mathscr{C}(\mathrm{t}) - \sigma\,\mathscr{B}(\mathrm{t}) - \mu\,\mathscr{B}(\mathrm{t});\\
&D_t^{\phi}\mathscr{C}(\mathrm{t}) = \sigma\,\mathscr{B}(\mathrm{t}) - \gamma\,\mathscr{C}(\mathrm{t}) - s\,\mathscr{C}(\mathrm{t}) - \mu\,\mathscr{I}(\mathrm{t});\\
&D_t^{\phi}\mathscr{Y}(\mathrm{t}) = s\,\mathscr{C}(\mathrm{t}) - \delta\,\mathscr{Y}(\mathrm{t}) - \mu\,\mathscr{Y}(\mathrm{t});\\
&D_t^{\phi}\mathscr{Z}(\mathrm{t}) = \delta\,\mathscr{Y}(\mathrm{t}) - r\,\mathscr{Z}(\mathrm{t}) - \mu\,\mathscr{Z}(\mathrm{t});\\
&D_t^{\phi}\mathscr{R}(\mathrm{t}) = \gamma\,\mathscr{C}(\mathrm{t}) + r\,\mathscr{Z}(\mathrm{t}) - \mu\,\mathscr{R}(\mathrm{t}).
\end{aligned} \tag{5}$$

Applying Laplace transform to both sides of the system of equation (1), and we have

$$\begin{aligned}
&\mathcal{L}\{\mathscr{A}(\mathrm{t})\} - \frac{1}{s}\mathscr{A}_0 - \frac{1}{\mathcal{B}(\phi)}\left(1-\phi+\frac{\phi}{s^{\phi}}\right)\mathcal{L}\left\{\theta - \beta\,\mathscr{A}(\mathrm{t})\,\mathscr{C}(\mathrm{t}) - \mu\,\mathscr{A}(\mathrm{t})\right\} = 0;\\
&\mathcal{L}\{\mathscr{B}(\mathrm{t})\} - \frac{1}{s}\mathscr{B}_0 - \frac{1}{\mathcal{B}(\phi)}\left(1-\phi+\frac{\phi}{s^{\phi}}\right)\mathcal{L}\left\{\beta\,\mathscr{A}(\mathrm{t})\,\mathscr{C}(\mathrm{t}) - \sigma\,\mathscr{B}(\mathrm{t}) - \mu\,\mathscr{B}(\mathrm{t})\right\} = 0;\\
&\mathcal{L}\{\mathscr{C}(\mathrm{t})\} - \frac{1}{s}\mathscr{C}_0 - \frac{1}{\mathcal{B}(\phi)}\left(1-\phi+\frac{\phi}{s^{\phi}}\right)\mathcal{L}\left\{\sigma\,\mathscr{B}(\mathrm{t}) - \gamma\,\mathscr{C}(\mathrm{t}) - s\,\mathscr{C}(\mathrm{t}) - \mu\,\mathscr{C}(\mathrm{t})\right\} = 0;\\
&\mathcal{L}\{\mathscr{Y}(\mathrm{t})\} - \frac{1}{s}\mathscr{Y}_0 - \frac{1}{\mathcal{B}(\phi)}\left(1-\phi+\frac{\phi}{s^{\phi}}\right)\mathcal{L}\left\{s\,\mathscr{C}(\mathrm{t}) - \delta\,\mathscr{Y}(\mathrm{t}) - \mu\,\mathscr{Y}(\mathrm{t})\right\} = 0;\\
&\mathcal{L}\{\mathscr{Z}(\mathrm{t})\} - \frac{1}{s}\mathscr{Z}_0 - \frac{1}{\mathcal{B}(\phi)}\left(1-\phi+\frac{\phi}{s^{\phi}}\right)\mathcal{L}\left\{\delta\,\mathscr{Y}(\mathrm{t}) - r\,\mathscr{Z}(\mathrm{t}) - \mu\,\mathscr{Z}(\mathrm{t})\right\} = 0;\\
&\mathcal{L}\{\mathscr{R}(\mathrm{t})\} - \frac{1}{s}\mathscr{R}_0 - \frac{1}{\mathcal{B}(\phi)}\left(1-\phi+\frac{\phi}{s^{\phi}}\right)\mathcal{L}\left\{\gamma\,\mathscr{C}(\mathrm{t}) + r\,\mathscr{Z}(\mathrm{t}) - \mu\,\mathscr{R}(\mathrm{t})\right\} = 0.
\end{aligned} \tag{6}$$

Define the non linear operator as,

$$\begin{aligned}
&\mathcal{N}^1[\vartheta_1,\vartheta_2,\vartheta_3,\vartheta_4,\vartheta_5,\vartheta_6]\\
&\quad = \mathcal{L}\{\vartheta_1(t;q)\} - \frac{1}{s}\mathscr{A}_0 - \frac{1}{\mathcal{B}(\phi)}\left(1-\phi+\frac{\phi}{s^{\phi}}\right)\mathcal{L}\{\theta - \beta\,\vartheta_1(t;q)\,\vartheta_3(t;q) - \mu\,\vartheta_1(t;q)\};\\
&\mathcal{N}^2[\vartheta_1,\vartheta_2,\vartheta_3,\vartheta_4,\vartheta_5,\vartheta_6]\\
&\quad = \mathcal{L}\{\vartheta_2(t;q)\} - \frac{1}{s}\mathscr{B}_0 - \frac{1}{\mathcal{B}(\phi)}\left(1-\phi+\frac{\phi}{s^{\phi}}\right)\mathcal{L}\{\beta\,\vartheta_1(t;q)\,\vartheta_3(t;q) - (\sigma+\mu)\,\vartheta_2(t;q)\};\\
&\mathcal{N}^3[\vartheta_1,\vartheta_2,\vartheta_3,\vartheta_4,\vartheta_5,\vartheta_6]\\
&\quad = \mathcal{L}\{\vartheta_3(t;q)\} - \frac{1}{s}\mathscr{C}_0 - \frac{1}{\mathcal{B}(\phi)}\left(1-\phi+\frac{\phi}{s^{\phi}}\right)\mathcal{L}\{\sigma\,\vartheta_2(\iota;q) - (\gamma+s+\mu)\,\vartheta_3(t;q)\};\\
&\mathcal{N}^4[\vartheta_1,\vartheta_2,\vartheta_3,\vartheta_4,\vartheta_5,\vartheta_6]\\
&\quad = \mathcal{L}\{\vartheta_4(t;q)\} - \frac{1}{s}\mathscr{Y}_0 - \frac{1}{\mathcal{B}(\phi)}\left(1-\phi+\frac{\phi}{s^{\phi}}\right)\mathcal{L}\{s\,\vartheta_3(t;q) - (\delta+\mu)\,\vartheta_4(t;q)\};
\end{aligned}$$

$$\mathcal{N}^5[\vartheta_1,\vartheta_2,\vartheta_3,\vartheta_4,\vartheta_5,\vartheta_6]$$
$$= \mathcal{L}\{\vartheta_5(t;q)\} - \frac{1}{s}\mathscr{Z}_0 - \frac{1}{\mathcal{B}(\phi)}\left(1-\phi+\frac{\phi}{s^\phi}\right)\mathcal{L}\{\delta\,\vartheta_4(t;q) - (r+\mu)\,\vartheta_5(t;q)\};$$
$$\mathcal{N}^6[\vartheta_1,\vartheta_2,\vartheta_3,\vartheta_4,\vartheta_5,\vartheta_6]$$
$$= \mathcal{L}\{\vartheta_6(t;q)\} - \frac{1}{s}\mathscr{R}_0 - \frac{1}{\mathcal{B}(\phi)}\left(1-\phi+\frac{\phi}{s^\phi}\right)\mathcal{L}\{\gamma\,\vartheta_3(t;q) + r\,\vartheta_5(t;q) - \mu\,\vartheta_6(t;q)\}. \tag{7}$$

The deformation equation of mth order is obtained by using the proposed approach as

$$\mathcal{L}[\mathscr{A}_m(\mathrm{t}) - K_m\mathscr{A}_{m-1}(\mathrm{t})] = \mathfrak{h}\,\Re_{1,m}[\vec{\mathscr{A}}_{m-1},\vec{\mathscr{B}}_{m-1},\vec{\mathscr{C}}_{m-1},\vec{\mathscr{Y}}_{m-1},\vec{\mathscr{Z}}_{m-1},\vec{\mathscr{R}}_{m-1}],$$
$$\mathcal{L}[\mathscr{B}_m(\mathrm{t}) - K_m\mathscr{B}_{m-1}(\mathrm{t})] = \mathfrak{h}\,\Re_{2,m}[\vec{\mathscr{A}}_{m-1},\vec{\mathscr{B}}_{m-1},\vec{\mathscr{C}}_{m-1},\vec{\mathscr{Y}}_{m-1},\vec{\mathscr{Z}}_{m-1},\vec{\mathscr{R}}_{m-1}],$$
$$\mathcal{L}[\mathscr{C}_m(\mathrm{t}) - K_m\mathscr{C}_{m-1}(\mathrm{t})] = \mathfrak{h}\,\Re_{3,m}[\vec{\mathscr{A}}_{m-1},\vec{\mathscr{B}}_{m-1},\vec{\mathscr{C}}_{m-1},\vec{\mathscr{Y}}_{m-1},\vec{\mathscr{Z}}_{m-1},\vec{\mathscr{R}}_{m-1}],$$
$$\mathcal{L}[\mathscr{Y}_m(\mathrm{t}) - K_m\mathscr{Y}_{m-1}(\mathrm{t})] = \mathfrak{h}\,\Re_{4,m}[\vec{\mathscr{A}}_{m-1},\vec{\mathscr{B}}_{m-1},\vec{\mathscr{C}}_{m-1},\vec{\mathscr{Y}}_{m-1},\vec{\mathscr{Z}}_{m-1},\vec{\mathscr{R}}_{m-1}],$$
$$\mathcal{L}[\mathscr{Z}_m(\mathrm{t}) - K_m\mathscr{Z}_{m-1}(\mathrm{t})] = \mathfrak{h}\,\Re_{5,m}[\vec{\mathscr{A}}_{m-1},\vec{\mathscr{B}}_{m-1},\vec{\mathscr{C}}_{m-1},\vec{\mathscr{Y}}_{m-1},\vec{\mathscr{Z}}_{m-1},\vec{\mathscr{R}}_{m-1}],$$
$$\mathcal{L}[\mathscr{R}_m(\mathrm{t}) - K_m\mathscr{R}_{m-1}(\mathrm{t})] = \mathfrak{h}\,\Re_{6,m}[\vec{\mathscr{A}}_{m-1},\vec{\mathscr{B}}_{m-1},\vec{\mathscr{C}}_{m-1},\vec{\mathscr{Y}}_{m-1},\vec{\mathscr{Z}}_{m-1},\vec{\mathscr{R}}_{m-1}],$$

where

$$\Re_{1,m}[vec\mathscr{A}_{m-1},\vec{\mathscr{B}}_{m-1},\vec{\mathscr{C}}_{m-1},\vec{\mathscr{Y}}_{m-1},\vec{\mathscr{Z}}_{m-1},\vec{\mathscr{R}}_{m-1}]$$
$$= \mathcal{L}\{\mathscr{A}_{m-1}(t)\} - \left(1-\frac{K_m}{\mathfrak{n}}\right)\frac{\mathscr{A}_0}{s} - \frac{1}{\mathcal{B}(\phi)}\left(1-\phi+\frac{\phi}{s^\phi}\right)\mathcal{L}\left\{\theta - \beta\sum_{i=0}^{m-1}\mathscr{A}_i(\mathrm{t})\,\mathscr{C}_{m-1-i}(\mathrm{t}) - \mu\,\mathscr{A}_{m-1}(\mathrm{t})\right\},$$
$$\Re_{2,m}[\vec{\mathscr{A}}_{m-1},\vec{\mathscr{B}}_{m-1},\vec{\mathscr{C}}_{m-1},\vec{\mathscr{Y}}_{m-1},\vec{\mathscr{Z}}_{m-1},\vec{\mathscr{R}}_{m-1}]$$
$$= \mathcal{L}\{\mathscr{B}_{m-1}(t)\} - \left(1-\frac{K_m}{\mathfrak{n}}\right)\frac{\mathscr{B}_0}{s} - \frac{1}{\mathcal{B}(\phi)}\left(1-\phi+\frac{\phi}{s^\phi}\right)\mathcal{L}\left\{\beta\sum_{i=0}^{m-1}\mathscr{A}_i(\mathrm{t})\,\mathscr{C}_{m-1-i}(\mathrm{t}) - (\sigma+\mu)\,\mathscr{B}_{m-1}(\mathrm{t})\right\},$$
$$\Re_{3,m}[\vec{\mathscr{A}}_{m-1},\vec{\mathscr{B}}_{m-1},\vec{\mathscr{C}}_{m-1},\vec{\mathscr{Y}}_{m-1},\vec{\mathscr{Z}}_{m-1},\vec{\mathscr{R}}_{m-1}]$$
$$= \mathcal{L}\{\mathscr{C}_{m-1}(t)\} - \left(1-\frac{K_m}{\mathfrak{n}}\right)\frac{\mathscr{C}_0}{s} - \frac{1}{\mathcal{B}(\phi)}\left(1-\phi+\frac{\phi}{s^\phi}\right)\mathcal{L}\{\sigma\mathscr{B}_{m-1}(\mathrm{t}) - (\gamma+s+\mu)\,\mathscr{C}_{m-1}(\mathrm{t})\},$$
$$\Re_{4,m}[\vec{\mathscr{A}}_{m-1},\vec{\mathscr{B}}_{m-1},\vec{\mathscr{C}}_{m-1},\vec{\mathscr{Y}}_{m-1},\vec{\mathscr{Z}}_{m-1},\vec{\mathscr{R}}_{m-1}]$$
$$= \mathcal{L}\{\mathscr{Y}_{m-1}(t)\} - \left(1-\frac{K_m}{\mathfrak{n}}\right)\frac{\mathscr{Y}_0}{s} - \frac{1}{\mathcal{B}(\phi)}\left(1-\phi+\frac{\phi}{s^\phi}\right)\mathcal{L}\{s\,\mathscr{C}_{m-1}(\mathrm{t}) - (\delta+\mu)\,\mathscr{Y}_{m-1}(\mathrm{t})\},$$
$$\Re_{5,m}[\vec{\mathscr{A}}_{m-1},\vec{\mathscr{B}}_{m-1},\vec{\mathscr{C}}_{m-1},\vec{\mathscr{Y}}_{m-1},\vec{\mathscr{Z}}_{m-1},\vec{\mathscr{R}}_{m-1}]$$
$$= \mathcal{L}\{\mathscr{Z}_{m-1}(t)\} - \left(1-\frac{K_m}{\mathfrak{n}}\right)\frac{\mathscr{Y}_0}{s} - \frac{1}{\mathcal{B}(\phi)}\left(1-\phi+\frac{\phi}{s^\phi}\right)\mathcal{L}\{\delta\,\mathscr{Y}_{m-1}(\mathrm{t}) - (r+\mu)\,\mathscr{Z}_{m-1}(\mathrm{t})\},$$
$$\Re_{6,m}[\vec{\mathscr{A}}_{m-1},\vec{\mathscr{B}}_{m-1},\vec{\mathscr{C}}_{m-1},\vec{\mathscr{Y}}_{m-1},\vec{\mathscr{Z}}_{m-1},\vec{\mathscr{R}}_{m-1}]$$
$$= \mathcal{L}\{\mathscr{R}_{r-1}(t)\} - \left(1-\frac{K_m}{\mathfrak{n}}\right)\frac{\mathscr{Y}_0}{s} - \frac{1}{\mathcal{B}(\phi)}\left(1-\phi+\frac{\phi}{s^\phi}\right)\mathcal{L}\{\gamma\,\mathscr{C}_{m-1}(\mathrm{t}) + r\,\mathscr{Z}_{m-1}(\mathrm{t}) - \mu\,\mathscr{R}_{m-1}(\mathrm{t})\}.$$

Applying the inverse Laplace transform to the deformation equation, the system yields

$$\mathscr{A}_m(\mathrm{t}) = K_m\,\mathscr{A}_{m-1}(\mathrm{t}) + \mathfrak{h}\,\mathcal{L}^{-1}\{\Re_{1,m}[\vec{\mathscr{A}}_{m-1},\vec{\mathscr{B}}_{m-1},\vec{\mathscr{C}}_{m-1},\vec{\mathscr{Y}}_{m-1},\vec{\mathscr{Z}}_{m-1},\vec{\mathscr{R}}_{m-1}]\},$$
$$\mathscr{B}_m(\mathrm{t}) = K_m\,{}_{m-1}(\mathrm{t}) + \mathfrak{h}\,\mathcal{L}^{-1}\{\Re_{2,m}[\vec{\mathscr{A}}_{m-1},\vec{\mathscr{B}}_{m-1},\vec{\mathscr{C}}_{m-1},\vec{\mathscr{Y}}_{m-1},\vec{\mathscr{Z}}_{m-1},\vec{\mathscr{R}}_{m-1}]\},$$
$$\mathscr{C}_m(\mathrm{t}) = K_m\,\mathscr{C}_{m-1}(\mathrm{t}) + \mathfrak{h}\,\mathcal{L}^{-1}\{\Re_{3,m}[\vec{\mathscr{A}}_{m-1},\vec{\mathscr{B}}_{m-1},\vec{\mathscr{C}}_{m-1},\vec{\mathscr{Y}}_{m-1},\vec{\mathscr{Z}}_{m-1},\vec{\mathscr{R}}_{m-1}]\},$$

$$\mathscr{Y}_m(t) = K_m\,\mathscr{Y}_{m-1}(t) + \hbar\,\mathcal{L}^{-1}\{\Re_{4,m}[\vec{\mathscr{A}}_{m-1}, \vec{\mathscr{B}}_{m-1}, \vec{\mathscr{C}}_{m-1}, \vec{\mathscr{Y}}_{m-1}, \vec{\mathscr{Z}}_{m-1}, \vec{\mathscr{R}}_{m-1}]\},$$
$$\mathscr{Z}_m(t) = K_m\,\mathscr{Z}_{m-1}(t) + \hbar\,\mathcal{L}^{-1}\{\Re_{5,m}[\vec{\mathscr{A}}_{m-1}, \vec{\mathscr{B}}_{m-1}, \vec{\mathscr{C}}_{m-1}, \vec{\mathscr{Y}}_{m-1}, \vec{\mathscr{Z}}_{m-1}, \vec{\mathscr{R}}_{m-1}]\},$$
$$\mathscr{R}_m(t) = K_m\,\mathscr{R}_{m-1}(t) + \hbar\,\mathcal{L}^{-1}\{\Re_{6,m}[\vec{\mathscr{A}}_{m-1}, \vec{\mathscr{B}}_{m-1}, \vec{\mathscr{C}}_{m-1}, \vec{\mathscr{Y}}_{m-1}, \vec{\mathscr{Z}}_{m-1}, \vec{\mathscr{R}}_{m-1}]\}. \tag{8}$$

On solving eq. (8), and using initial conditions, we obtain

$$\mathscr{A}_0(t) = 34218169,$$
$$\mathscr{B}_0(t) = 5000,$$
$$\mathscr{C}_0(t) = 1720,$$
$$\mathscr{Y}_0(t) = 157,$$
$$\mathscr{Z}_0(t) = 120,$$
$$\mathscr{R}_0(t) = 99,$$
$$\mathscr{A}_1(t) = \frac{-1155.744429\,\hbar}{\mathcal{B}(\phi)}\left\{1-\phi+\frac{\phi\,t^{\phi}}{\Gamma(\phi+1)}\right\},$$
$$\mathscr{B}_1(t) = \frac{-67.56050140\,\hbar}{\mathcal{B}(\phi)}\left\{1-\phi+\frac{\phi\,t^{\phi}}{\Gamma(\phi+1)}\right\},$$
$$\mathscr{C}_1(t) = \frac{-37.90840000\,\hbar}{\mathcal{B}(\phi)}\left\{1-\phi+\frac{\phi\,t^{\phi}}{\Gamma(\phi+1)}\right\},$$
$$\mathscr{Y}_1(t) = \frac{-7.967290000\,\hbar}{\mathcal{B}(\phi)}\left\{1-\phi+\frac{\phi\,t^{\phi}}{\Gamma(\phi+1)}\right\},$$
$$\mathscr{Z}_1(t) = \frac{-0.5044000000\,\hbar}{\mathcal{B}(\phi)}\left\{1-\phi+\frac{\phi\,t^{\phi}}{\Gamma(\phi+1)}\right\},$$
$$\mathscr{R}_1(t) = \frac{-3.557030000\,\hbar}{\mathcal{B}(\phi)}\left\{1-\phi+\frac{\phi\,t^{\phi}}{\Gamma(\phi+1)}\right\},$$
$$\begin{aligned}\mathscr{A}_2(t) = {} & \frac{-1155.744429\,\hbar\,(\mathfrak{n}+\hbar)}{\mathcal{B}(\phi)}\left\{1-\phi+\frac{\phi\,t^{\phi}}{\Gamma(\phi+1)}\right\} \\ & - \frac{2.632960169\,\hbar^2}{[\mathcal{B}(\phi)]^2}\left(1-2\phi+\phi^2+\frac{2\phi\,(1-\phi)\,t^{\phi}}{\Gamma(\phi+1)}+\frac{\phi^2\,t^{2\phi}}{\Gamma(2\phi+1)}\right) \\ & - \frac{2300\,\hbar}{\mathcal{B}(\phi)}\left\{1-\phi+\frac{\phi\,t^{\phi}}{\Gamma(\phi+1)}\right\},\end{aligned}$$
$$\begin{aligned}\mathscr{B}_2(t) = {} & \frac{-67.56050140\,\hbar\,(\mathfrak{n}+\hbar)}{\mathcal{B}(\phi)}\left\{1-\phi+\frac{\phi\,t^{\phi}}{\Gamma(\phi+1)}\right\} \\ & + \frac{1.920656007\,\hbar^2}{[\mathcal{B}(\phi)]^2}\left(1-2\phi+\phi^2+\frac{2\phi\,(1-\phi)\,t^{\phi}}{\Gamma(\phi+1)}+\frac{\phi^2\,t^{2\phi}}{\Gamma(2\phi+1)}\right),\end{aligned}$$
$$\begin{aligned}\mathscr{C}_2(t) = {} & \frac{-37.90840000\,\hbar\,(\mathfrak{n}+\hbar)}{\mathcal{B}(\phi)}\left\{1-\phi+\frac{\phi\,t^{\phi}}{\Gamma(\phi+1)}\right\} \\ & + \frac{0.4091089620\,\hbar^2}{[\mathcal{B}(\phi)]^2}\left(1-2\phi+\phi^2+\frac{2\phi\,(1-\phi)\,t^{\phi}}{\Gamma(\phi+1)}+\frac{\phi^2\,t^{2\phi}}{\Gamma(2\phi+1)}\right),\end{aligned}$$
$$\begin{aligned}\mathscr{Y}_2(t) = {} & \frac{-7.967290000\,\hbar\,(\mathfrak{n}+\hbar)}{\mathcal{B}(\phi)}\left\{1-\phi+\frac{\phi\,t^{\phi}}{\Gamma(\phi+1)}\right\} \\ & + \frac{0.1574338213\,\hbar^2}{[\mathcal{B}(\phi)]^2}\left(1-2\phi+\phi^2+\frac{2\phi\,(1-\phi)\,t^{\phi}}{\Gamma(\phi+1)}+\frac{\phi^2\,t^{2\phi}}{\Gamma(2\phi+1)}\right),\end{aligned}$$

$$\mathscr{Z}_2(\mathrm{t}) = \frac{-7.967290000\,\mathfrak{h}\,(\mathfrak{n}+\mathfrak{h})}{\mathcal{B}(\phi)}\left\{1-\phi+\frac{\phi\,t^{\phi}}{\Gamma(\phi+1)}\right\} + \frac{0.03134962800\,\mathfrak{h}^2}{[\mathcal{B}(\phi)]^2}\left(1-2\phi+\phi^2+\frac{2\phi\,(1-\phi)\,t^{\phi}}{\Gamma(\phi+1)}+\frac{\phi^2\,t^{2\phi}}{\Gamma(2\phi+1)}\right),$$

$$\mathscr{R}_2(\mathrm{t}) = \frac{-7.967290000\,\mathfrak{h}\,(\mathfrak{n}+\mathfrak{h})}{\mathcal{B}(\phi)}\left\{1-\phi+\frac{\phi\,t^{\phi}}{\Gamma(\phi+1)}\right\} + \frac{0.7621448910\,\mathfrak{h}^2}{[\mathcal{B}(\phi)]^2}\left(1-2\phi+\phi^2+\frac{2\phi\,(1-\phi)\,t^{\phi}}{\Gamma(\phi+1)}+\frac{\phi^2\,t^{2\phi}}{\Gamma(2\phi+1)}\right), \tag{9}$$

and so forth, making the aforementioned set of equations simpler so that the values are obtained. As described by the solutions of the q-HATM, we obtain the series as follows:

$$\begin{aligned}
\mathscr{A}(\mathrm{t}) &= \mathscr{A}_0(\mathrm{t}) + \sum_{n=1}^{\infty} \mathscr{A}_m(\mathrm{t})\left(\frac{1}{\mathfrak{m}}\right)^n;\\
\mathscr{B}(\mathrm{t}) &= \mathscr{B}_0(\mathrm{t}) + \sum_{n=1}^{\infty} \mathscr{B}_m(\mathrm{t})\left(\frac{1}{\mathfrak{m}}\right)^n;\\
\mathscr{C}(\mathrm{t}) &= \mathscr{C}_0(\mathrm{t}) + \sum_{n=1}^{\infty} \mathscr{C}_m(\mathrm{t})\left(\frac{1}{\mathfrak{m}}\right)^n;\\
\mathscr{Y}(\mathrm{t}) &= \mathscr{Y}_0(\mathrm{t}) + \sum_{n=1}^{\infty} \mathscr{Y}_m(\mathrm{t})\left(\frac{1}{\mathfrak{m}}\right)^n;\\
\mathscr{Z}(\mathrm{t}) &= \mathscr{Z}_0(\mathrm{t}) + \sum_{n=1}^{\infty} \mathscr{Z}_m(\mathrm{t})\left(\frac{1}{\mathfrak{m}}\right)^n;\\
\mathscr{R}(\mathrm{t}) &= \mathscr{R}_0(\mathrm{t}) + \sum_{n=1}^{\infty} \mathscr{R}_m(\mathrm{t})\left(\frac{1}{\mathfrak{m}}\right)^n.
\end{aligned} \tag{10}$$

5. Results and Discussion

In this study, initially we employed the Hartman-Grobman theorem to analyze the stability conditions of a six-compartment model representing the dynamics of monkeypox transmission. The compartments included susceptible individuals (A), exposed individuals (B), infectious individuals (C), those experiencing systemic issues (Y), individuals with rash symptoms (Z), and recovered individuals (R). The initial values for these compartments were set as follows: $\mathscr{A}(0) = 34218169$, $\mathscr{B}(0) = 5000$, $\mathscr{C}(0) = 1720$, $\mathscr{Y}(0) = 157$, $\mathscr{Z}(0) = 120$, $\mathscr{R}(0) = 99$. Through our analysis, we established the local stability of the disease free equilibrium and identified conditions under which the disease could persist within the population. This provided valuable insights into the potential impact of interventions aimed at reducing transmission rates and controlling outbreaks. To further investigate the dynamics of monkeypox spread, we applied the q-homotopy analysis transform method (q-HATM) in conjunction with Maple software to generate comprehensive graphs and tables illustrating the behavior of the model this approach demonstrated a nuanced understanding of the interaction between compartments, revealing critical thresholds for intervention strategies. For instance, our findings indicated that increasing recovery rates among susceptible individuals significantly reduced the number of new infections and subsequent cases of systemic issues and rash. Moreover, the graphical representations highlighted the importance of timely responses to emerging cases, emphasizing

that early intervention can lead to a substantial decrease in overall morbidity. This study underscores the necessity for ongoing surveillance and adaptive public health strategies to mitigate the impact of monkeypox outbreaks effectively. The findings collected indicate that the suggested scheme is useful for comprehending behavior using fractional derivatives.

Table 1. The susceptible class table for $\mathscr{A}(t)$ for different ϕ values

t	$\phi = 0.6$	$\phi = 0.7$	$\phi = 0.8$	$\phi = 0.9$	$\phi = 1$
0	3.421955088×10^7	3.421920548×10^7	3.421886004×10^7	3.421851454×10^7	3.4218169×10^7
20	3.423351362×10^7	3.424080224×10^7	3.425131607×10^7	3.426616153×10^7	3.428675730×10^7
40	3.424068996×10^7	3.425421967×10^7	3.427518570×10^7	3.430697526×10^7	3.435429241×10^7
60	3.424648689×10^7	3.426563216×10^7	3.429653902×10^7	3.434531567×10^7	3.442077434×10^7
80	3.425153548×10^7	3.427590187×10^7	3.431637231×10^7	3.438201512×10^7	3.448620308×10^7
100	3.425609060×10^7	3.428539222×10^7	3.433512475×10^7	3.441745880×10^7	3.455057864×10^7
120	3.426028674×10^7	3.429430067×10^7	3.435304250×10^7	3.445187035×10^7	3.461390102×10^7

Table 2. The exposed class table for $\mathscr{B}(t)$ for different ϕ values

t	$\phi = 0.6$	$\phi = 0.7$	$\phi = 0.8$	$\phi = 0.9$	$\phi = 1$
0	5027.331506	5020.441009	5013.588926	5006.775257	5000
20	5330.161135	5501.653349	5762.101374	6153.104751	6735.341229
40	5504.196706	5853.125042	6450.717532	7475.409310	9238.944862
60	5653.977777	6184.189703	7168.079332	9012.955866	12510.81090
80	5791.158515	6507.604085	7921.662046	10760.82131	16550.93933
100	5920.339480	6828.155280	8712.807006	12712.78493	21359.33018
120	6043.900816	7148.166553	9541.291714	14863.15746	26935.98342

Table 3. The infected class table for $\mathscr{C}(t)$ for different ϕ values

t	$\phi = 0.6$	$\phi = 0.7$	$\phi = 0.8$	$\phi = 0.9$	$\phi = 1$
0	1735.228817	1731.409340	1727.598044	1723.794931	1720
20	1895.026173	1981.420208	2108.946365	2294.176764	2559.989792
40	1981.240863	2148.406273	2420.083834	2858.351765	3563.623170
60	2052.926568	2297.571906	2720.927783	3453.937487	4730.900132
80	2116.853902	2437.464308	3019.741690	4085.357121	6061.820678
100	2175.734020	2571.555502	3319.734250	4753.782097	7556.384810
120	2230.986883	2701.670056	3622.487449	5459.431115	9214.592526

Table 4. The systemic issue class table for $\mathscr{Y}(t)$ for different ϕ values

t	$\phi = 0.6$	$\phi = 0.7$	$\phi = 0.8$	$\phi = 0.9$	$\phi = 1$
0	160.2121054	159.4043560	158.5997554	157.7983033	157
20	194.8787139	214.0869429	242.8784472	285.4596783	347.8325643
40	214.2209282	252.4129766	316.3125044	423.0321852	601.6386570
60	230.6078437	287.6744089	390.4069419	576.7564500	918.4182783
80	245.4377226	321.5191450	466.4636516	746.7941868	1298.171428
100	259.2665060	354.5929103	544.8945327	932.8933823	1740.898106
120	272.3836044	387.2235024	625.8496664	1134.735474	2246.598313

Table 5. The rash class table for $\mathscr{Z}(t)$ for different ϕ values

t	$\phi = 0.6$	$\phi = 0.7$	$\phi = 0.8$	$\phi = 0.9$	$\phi = 1$
0	120.2067759	120.1541415	120.1021340	120.0507535	120
20	122.7251810	124.2556430	126.6736563	130.4620316	136.3579256
40	124.3155029	127.6487116	133.7292638	144.8572249	165.2557024
60	125.7481428	131.0514911	141.6717423	163.1329827	206.6933304
80	127.1042215	134.5238736	150.4533745	185.0697317	260.6708096
100	128.4147848	138.0816022	160.0216864	210.5024187	327.1881400
120	129.6954538	141.7287672	170.3315908	239.3017854	406.2453216

Table 6. The recovered class table for $\mathscr{R}(t)$ for different ϕ values

t	$\phi = 0.6$	$\phi = 0.7$	$\phi = 0.8$	$\phi = 0.9$	$\phi = 1$
0	100.4350063	100.0739683	99.71445458	99.35646514	99
20	116.0017924	124.66454470	137.6836437	156.9970946	185.3834978
40	124.7386054	142.0433399	171.1357156	219.9930341	302.2527913
60	132.1641669	158.1104064	205.1168775	290.9922653	449.6078804
80	138.9006851	173.5891404	240.1722885	370.0032798	627.4487651
100	145.1952117	188.7608605	276.46406764	456.8722340	835.7754455
120	151.1762067	203.7672944	314.0440868	551.4266628	1074.587922

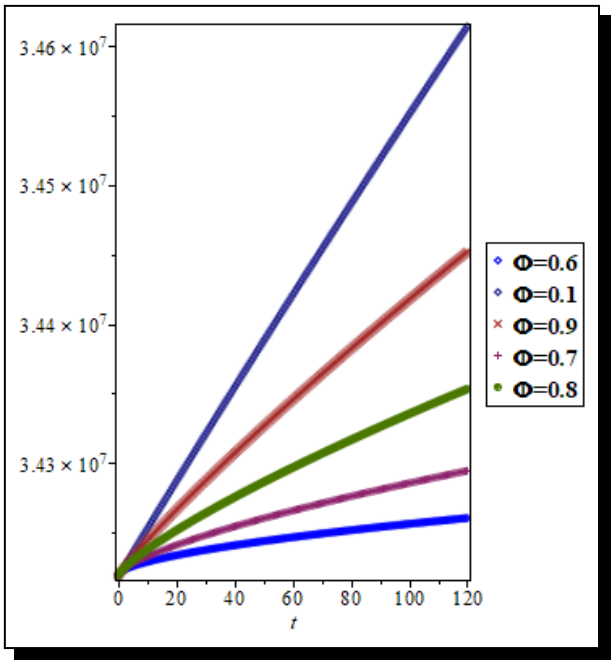

Figure 1. Plot of q-HATM solution for $\mathscr{A}(t)$ with respect to t at $\mathfrak{h} = -1$, $\mathfrak{m} = 1$, for varying ϕ

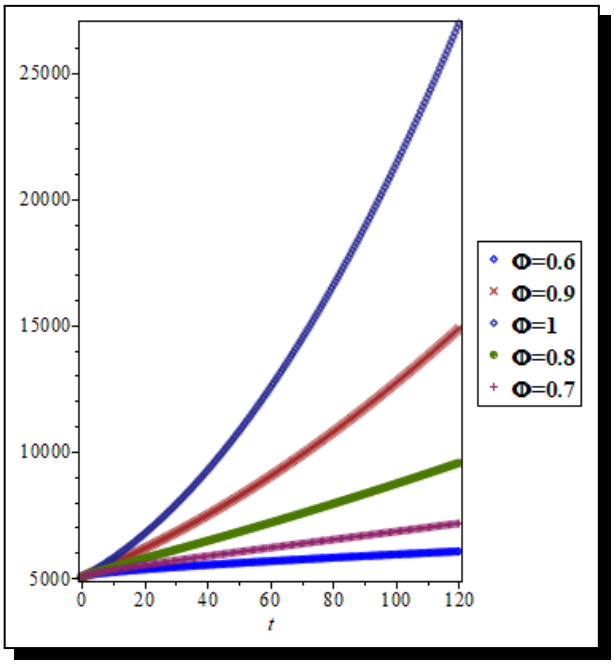

Figure 2. Plot of q-HATM solution for $\mathscr{B}(t)$ with respect to t at $\mathfrak{h} = -1$, $\mathfrak{m} = 1$, for varying ϕ

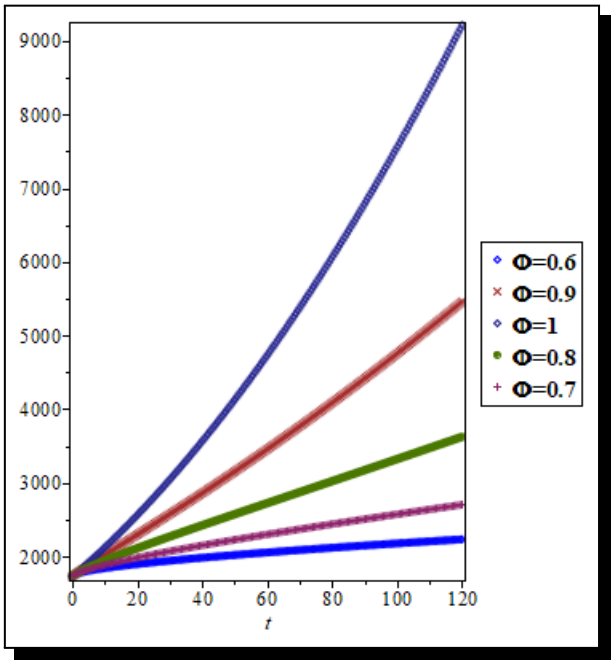

Figure 3. Plot of q-HATM solution for $\mathscr{C}(t)$ with respect to t at $\mathfrak{h} = -1$, $\mathfrak{m} = 1$, for varying ϕ

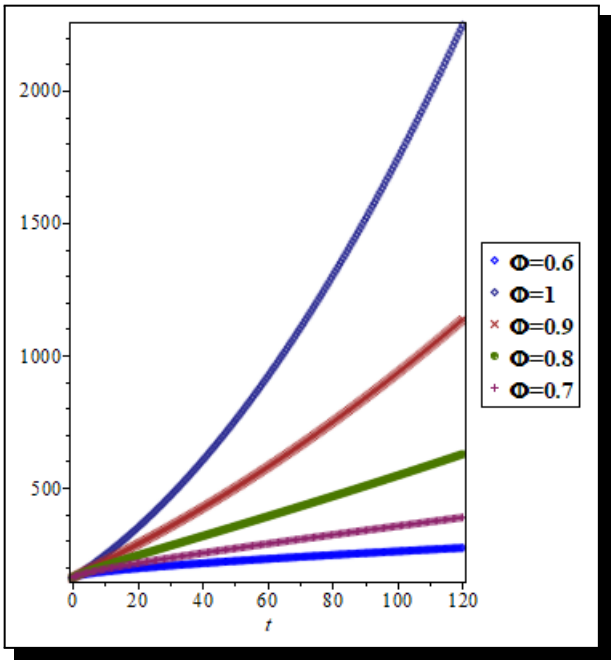

Figure 4. Plot of q-HATM solution for $\mathscr{D}(t)$ with respect to t at $\mathfrak{h} = -1$, $\mathfrak{m} = 1$, for varying ϕ

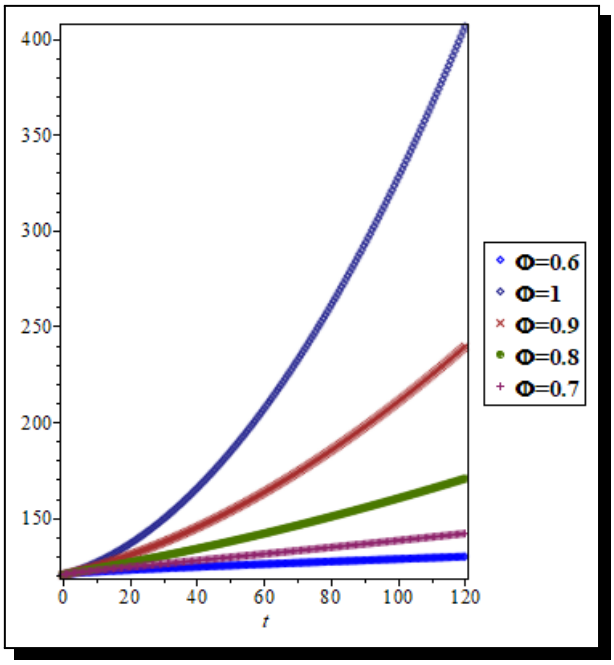

Figure 5. Plot of q-HATM solution for $\mathscr{Z}(\mathfrak{t})$ with respect to $\mathfrak{t}$ at $\mathfrak{h} = -1$, $\mathfrak{m} = 1$, for varying ϕ

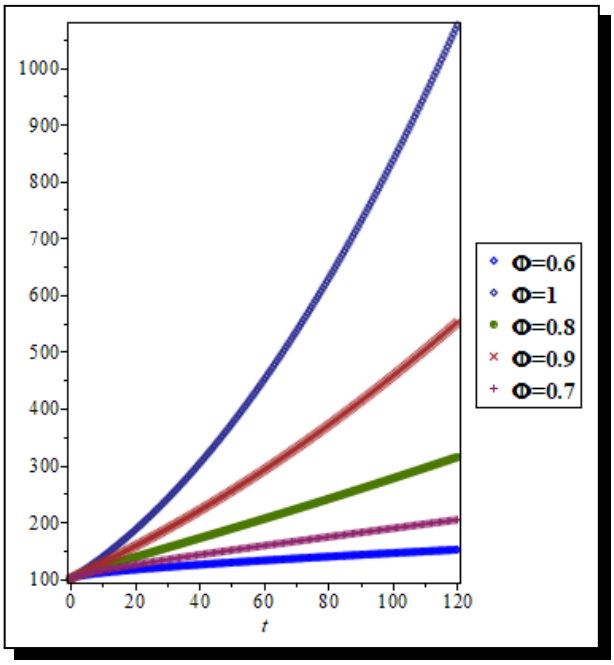

Figure 6. Plot of q-HATM solution for $\mathscr{R}(\mathfrak{t})$ with respect to $\mathfrak{t}$ at $\mathfrak{h} = -1$, $\mathfrak{m} = 1$, for varying ϕ

6. Conclusion

This study provides a entire analysis of monkeypox transmission dynamics through the development and application of a six compartment model. By leveraging the Hartman Grobman theorem, we established the local stability of the disease free equilibrium and identified critical conditions for disease persistence. The application of the q-Homotopy Analysis Transform Method further enhanced our understanding of the models behavior over time, revealing key insights into the interaction among compartments. Our findings underscore the significant impact of targeted interventions, such as increasing recovery rates among susceptible individuals, on reducing transmission and controlling outbreaks. The graphical analyses highlighted the importance of timely public health response to emerging cases, emphasizing that early intervention can substantially mitigate morbidity associated with monkeypox. We conclude that the suggested method is more scientific and successful, and that it may be applied to the study of nonlinear fractional mathematical models that describe biological phenomena. Additionally, the application of fractional calculus offers up new possibilities for mathematical modelling.

Competing Interests

The authors declare that they have no competing interests.

Authors' Contributions

All the authors contributed significantly in writing this article. The authors read and approved the final manuscript.

References

[1] M. Abdullah, A. Ahmad, N. Raza, M. Farman and M. O. Ahmad, Approximate solution and analysis of smoking epidemicmodel with Caputo fractional derivatives, *International Journal of Applied and Computational Mathematics* **4** (2018), article number 112, DOI: 10.1007/s40819-018-0543-5.

[2] E. Alkunle, U. Moens, G. Nehinda and M. Okeke, Monkeypox virus in Nigeria: Infection biology, epidemiology, and evolution, *Viruses* **12**(11) (2020), 1257, DOI: 10.3390/v12111257.

[3] E. Alzahrani and A. Zeb, Stability analysis and prevention strategies of tobacco smoking model, *Boundary Value Problems* **2020** (2020), Article number: 3, DOI: 10.1186/s13661-019-01315-1.

[4] A. Atangana and J. F. Gómez-Aguilar, A new derivative with normal distribution kernel: Theory, methods and applications, *Physica A: Statistical Mechanics and its Applications* **476** (2017), 1 – 14, DOI: 10.1016/j.physa.2017.02.016.

[5] A. Atangana and J. F. Gómez-Aguilar, Hyperchaotic behaviour obtained via a nonlocal operator with exponential decay and Mittag-Leffler laws, *Chaos, Solitons & Fractals* **102** (2017), 285 – 294, DOI: 10.1016/j.chaos.2017.03.022.

[6] C. P. Bhunu and S. Mushayabasa, Modelling the transmission dynamics of pox-like infections, *IAENG International Journal of Applied Mathematics* **41**(2) (2011), 9 pages, URL: https://www.iaeng.org/IJAM/issues_v41/issue_2/IJAM_41_2_09.pdf.

[7] G. Chowell, N. W. Hengartner, C. Castillo-Chavez, P. W. Fenimore and J. M. Hyman, The basic reproductive number of Ebola and the effects of public health measures: The cases of Congo and Uganda, *Journal of Theoretical Biology* **229**(1) (2004), 119 – 126, DOI: 10.1016/j.jtbi.2004.03.006.

[8] G. Hobson, J. Adamson, H. Adler, R. Firth, S. Gould, C. Houlihan, C. Johnson, D. Porter, T. Rampling, L. Ratcliffe, K. Russell, A. G. Shankar and T. Wingfield, Family cluster of three cases of monkeypox imported from Nigeria to the United Kingdom, May 2021, *Eurosurveillance* **26**(32) (2021), 2100745, DOI: 10.2807/1560-7917.ES.2021.26.32.2100745.

[9] H.-F. Huo, R. Chen and X.-Y. Wang, Modelling and stability of HIV/AIDS epidemic model with treatment, *Applied Mathematical Modelling* **40**(13-14) (2016), 6550 – 6559, DOI: 10.1016/j.apm.2016.01.054.

[10] R. F. Johnson, S. Yellayi, J. A. Cann, A. Johnson, A. L. Smith, J. Paragas, P. B. Jahrling and J. E. Blaney, Cowpox virus infection of cynomolgus macaques as a model of hemorrhagic smallpox, *Virology* **418**(2) (2011), 102 – 102, DOI: 10.1016/j.virol.2011.07.013.

[11] K. M. Owolabi and A. Atangana, Mathematical analysis and computational experiments for an epidemic system with nonlocal and nonsingular derivative, *Chaos, Solitons & Fractals* **126** (2019), 41 – 49, DOI: 10.1016/j.chaos.2019.06.001.

[12] V. Padmavathi, N. Magesh, K. Alagesan, M. I. Khan, S. Elattar, M. Alwetaishi and A. M. Galal, Numerical modeling and symmetry analysis of a pine wilt disease Model using the Mittag-Leffler kernel, *Symmetry* **14**(5) (2022), 1067, DOI: 10.3390/sym14051067.

[13] V. Padmavathi, A. Prakash, K. Alagesan and N. Magesh, Analysis and numerical simulation of novel coronavirus (COVID-19) model with Mittag-Leffler Kernel, *Mathematical Methods in the Applied Sciences* **44**(2) (2021), 1863 – 1877, DOI: 10.1002/mma.6886.

[14] S. Pathak, A. Maiti and G. P. P. Samanta, Rich dynamics of an SIR epidemic model, *Nonlinear Analysis: Modelling and Control*, **15**(1) (2010), 71 – 81, DOI: 10.15388/NA.2010.15.1.14365.

[15] A. Prakash and H. Kaur, Numerical solution for fractional model of Fokker-Planck equation by using q-HATM, *Chaos Solitons & Fractals* **105** (2017), 99 – 110, DOI: 10.1016/j.chaos.2017.10.003.

[16] A. Prakash and H. Kaur, Analysis and numerical simulation of fractional order Cahn-Allen model with Atangana-Baleanu derivative, *Chaos, Solitons & Fractals* **124** (2019), 134 – 142, DOI: 10.1016/j.chaos.2019.05.005.

[17] A. Prakash, M. Goyal, H. M. Baskonus and S. Gupta, A reliable hybrid numerical method for a time dependent vibration model of arbitrary order, *AIMS Mathematics* **5**(2) (2020), 979 – 1000, DOI: 10.3934/math.2020068.

[18] M. G. Reynolds, J. B. Doty, A. M. Mccollum, V. A. Olson and Y. Nakazawa, Monkeypox re-emergence in Africa: A call to expand the concept and practice of one health, *Expert Review of Anti-infective Therapy* **17**(2) (2019), 129 – 139, DOI: 10.1080/14787210.2019.1567330.

[19] J. Singh, D. Kumar and D. Baleanu, New aspects of fractional Biswas-Milovic model with Mittag-Leffler law, *Mathematical Modelling of Natural Phenomena* **14**(3) (2019), Article number 303, 23 pages, DOI: 10.1051/mmnp/2018068.

[20] S. A. Somma, N. I. Akinwande and U. D. Chado, A mathematical model of monkeypox virus transmission dynamics, *Ife Journal of Science* **21**(1) (2019), 195 – 204, DOI: 10.4314/ijs.v21i1.17.

[21] J. P. Thornhill, S. Barkati, S. Walmsley, J. Rockstroh, A. Antinori, L. B. Harrison, R. Palich, A. Nori, I. Reeves, M. S. Habibi, V. Apea, C. Boesecke, L. Vandekerckhove, M. Yakubovsky, E. Sendagorta, J. L. Blanco, E. Florence, D. Moschese, F. M. Maltez, A. Goorhuis, V. Pourcher, P. Migaud, S. Noe, C. Pintado, F. Maggi, A.-B. E. Hansen, C. Hoffmann, J. I. Lezama, C. Mussini, A. M. Cattelan, K. Makofane, D. Tan, S. Nozza, J. Nemeth, M. B. Klein and C. M. Orkin, Monkeypox Virus Infection in Humans across 16 Countries — April-June 2022, *New England Journal of Medicine* **387**(8) (2022), 679 – 691, DOI: 10.1056/NEJMoa2207323.

[22] P. Veeresha, D. G. Prakasha and H. M. Baskonus, Solving smoking epidemic model of fractional order using a modified homotopy analysis transform method, *Mathematical Sciences* **13**(2) (2019), 115 – 128, DOI: 10.1007/s40096-019-0284-6.

[23] P. Veeresha, D. G. Prakasha, N. Magesh, A. J. Christopher and D. U. Sarwe, Solution for fractional potential KdV and Benjamin equations using the novel technique, *Journal of Ocean Engineering and Science* **6**(3) (2021), 265 – 275, DOI: 10.1016/j.joes.2021.01.003.

[24] R. Vivancos, C. Anderson, P. Blomquist, S. Balasegaram, A. Bell, L. Bishop, C. S. Brown, Y. Chow, O. Edeghere, I. Florence, S. Logan, P. Manley, W. Crowe, A. McAuley, A. G. Shankar, B. Mora-Peris, K. Paranthaman, M. Prochazka, C. Ryan, D. Simons, R. Vipond, C. Byers, N. A. Watkins, UKHSA Monkeypox Incident Management Team10, W. Welfare, E. Whittaker, C. Dewsnap, A. Wilson, Y. Young, M. Chand, S. Riley and S. Hopkins, Community transmission of monkeypox in the United Kingdom, April to May 2022, *Eurosurveillance* **22** (27) (2022),5 pages, URL: https://www.eurosurveillance.org/content/10.2807/1560-7917.ES.2022.27.22.2200422.

[25] H. M. Youssef, N. Alahamdi, M. A. Ezzat, A. A. Elbary and A. M. Shawky, A proposed modified SEIQR epidemic model to analyze the COVID-19 spreading in Saudi Arabia, *Alexandria Engineering Journal* **61**(3) (2022), 2456 – 2470, DOI: 10.1016/j.aej.2021.06.095.